Journal of Alloys and Compounds 509 (2011) 466–470

Contents lists available at ScienceDirect

Journal of Alloys and Compounds

journal homepage: www.elsevier.com/locate/jallcom

Microstructure, ferroelectric, and piezoelectric properties of $(1-x-y)Bi_{0.5}Na_{0.5}TiO_3$–$xBaTiO_3$–$yBi_{0.5}Ag_{0.5}TiO_3$ lead-free ceramics

Lang Wu[a,*], Dingquan Xiao[b], Fei Zhou[a], Yuancheng Teng[a], Yuxiang Li[a]

[a] State Key Laboratory Cultivation Base for Nonmetal Composites and Functional Materials, Southwest University of Science and Technology, Mianyang 621010, China
[b] School of Material Science and Engineering, Sichuan University, Chengdu 610064, China

ARTICLE INFO

Article history:
Received 28 June 2010
Received in revised form 6 September 2010
Accepted 8 September 2010
Available online 22 September 2010

Keywords:
Ceramics
Microstructure
Ferroelectrics
Piezoelectricity

ABSTRACT

Lead-free $(1-x-y)Bi_{0.5}Na_{0.5}TiO_3$–$xBaTiO_3$–$yBi_{0.5}Ag_{0.5}TiO_3$ (BNT–BT–BAT-x/y, x = 0–0.10, y = 0–0.075) piezoelectric ceramics were synthesized by conventional oxide-mixed method. The microstructure, ferroelectric, and piezoelectric properties of the ceramics were investigated. Results show that a morphotropic phase boundary (MPB) between rhombohedral and tetragonal phases of BNT–BT–BAT-x/0.04 ceramics is formed at x = 0.06–0.08. The addition of BAT has no obvious change on the crystal structure of BNT–BT ceramics while it causes the grain size of the ceramics to become more homogenous. Near the MPB, the ceramics with x = 0.06 and y = 0.05–0.06 possess optimum electrical properties: $P_r \sim 42.5\ \mu C/cm^2$, $E_c \sim 32.0$ kV/cm, $d_{33} \sim 172$ pC/N, $k_p \sim 32.6\%$, and $k_t \sim 52.6\%$. The temperature dependences of k_p and polarization versus electric hysteresis loops reveal that the depolarization temperature (T_d) of BNT–BT–BAT-0.06/y ceramics decreases with increasing y. In addition, the polar and non-polar phases may coexist in the BNT–BT–BAT-x/y ceramics above T_d.

1. Introduction

Lead based perovskite $Pb(Zr,Ti)O_3$ (PZT)-based piezoelectric ceramics have dominated the commercial market of piezoelectric devices over the past 50 years, owing to their excellent electrical properties. Recently, the demand of the sustainable development of the world and the environmental regulations has induced a new surge in developing lead-free piezoelectric ceramics to replace the PZT-based ones [1,2].

It is known that the high polarizability of Pb^{2+} on the A-site of perovskite structure is in many cases greatly enhanced by the presence of a stereochemically active electron lone pair. The Bi^{3+} is isoelectronic with Pb^{2+} and also shows a lone pair effect. This has led some researchers to look toward Bi-based perovskites as alternatives to the lead-based piezoelectric materials. $(Bi_{0.5}Na_{0.5})TiO_3$ (BNT) is considered to be an excellent candidate for lead-free piezoelectric ceramics because of its relatively large remnant polarization (P_r = 38 μC/cm^2) [3]. However, pure BNT ceramics are very difficult to pole because of their relatively high coercive field (E_c = 73 kV/cm) and their piezoelectric properties (d_{33} = 72.9 pC/N) are not desirable [4]. To decrease the coercive field and enhance piezoelectric properties, other perovskite ferroelectrics were added into BNT to form new BNT-based solid solutions, such as BNT–$BaTiO_3$ (BNT–BT) [5–7], BNT–$Bi_{0.5}K_{0.5}TiO_3$ (BNT–BKT) [8], BNT–$BiAlO_3$ [9], BNT–BT–$Bi_{0.5}Li_{0.5}TiO_3$ [10], BNT–$K_{0.5}Na_{0.5}NbO_3$ [11], and so on.

Grinberg and Rappe [12] have recently reported that the short covalent Ag–O bonds on perovskite A-site, which are created through the 0.5 Å off-centering displacement of Ag, are similar to the short covalent bonds in many Pb-based perovskites. Consequently, Ag-containing perovskite solid solutions show large polarization and piezoelectric responses owing to the large distortion of Ag on the A-site, such as $AgNbO_3$ system [13].

$Bi_{0.5}Ag_{0.5}TiO_3$ is a ferroelectric which exhibits an orthorhombic distortion of the cubic perovskite structure at room temperature [14,15]. However, it is very difficult to synthesize $Bi_{0.5}Ag_{0.5}TiO_3$ under normal conditions [15]. A previous report [16] has demonstrated that $Bi_{0.5}Ag_{0.5}TiO_3$-modified BNT–BKT ceramics possess the optimum piezoelectric properties (d_{33} = 160 pC/N, k_p = 30%, k_t = 42%) in the morphotropic phase boundary (MPB) region. In present work, $Bi_{0.5}Ag_{0.5}TiO_3$ was introduced into BNT–BT to form a ternary $(1-x-y)Bi_{0.5}Na_{0.5}TiO_3$–$xBaTiO_3$–$yBi_{0.5}Ag_{0.5}TiO_3$ (BNT–BT–BAT-x/y) system. The microstructure, ferroelectric, and piezoelectric properties of the BNT–BT–BAT-x/y ceramics were examined. The piezoelectric and ferroelectric properties of the ceramics were also studied as a function of temperature.

2. Experimental

The BNT–BT–BAT-x/y (x = 0–0.10, y = 0–0.075) ceramics were prepared by the conventional oxide-mixed method. Bi_2O_3 (99%), TiO_2 (98%), $BaCO_3$ (99%), Na_2CO_3

* Corresponding author. Tel.: +86 816 2419201; fax: +86 816 2419201.
E-mail address: lang.wu@163.com (L. Wu).

0925-8388/$ – see front matter © 2010 Elsevier B.V. All rights reserved.
doi:10.1016/j.jallcom.2010.09.062

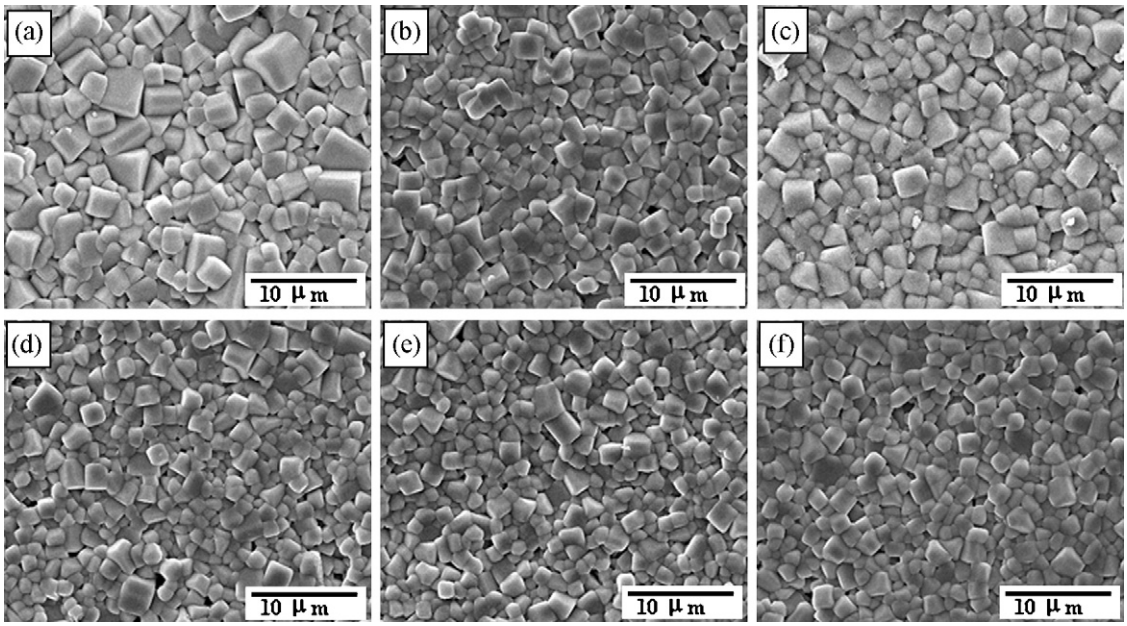

Fig. 1. SEM micrographs of (a) BNT–BT–BAT-0.04/0.04, (b) BNT–BT–BAT-0.08/0.04, (c) BNT–BT–BAT-0.10/0.04, (d) BNT–BT–BAT-0.06/0.00, (e) BNT–BT–BAT-0.06/0.04, and (f) BNT–BT–BAT-0.06/0.06 ceramics.

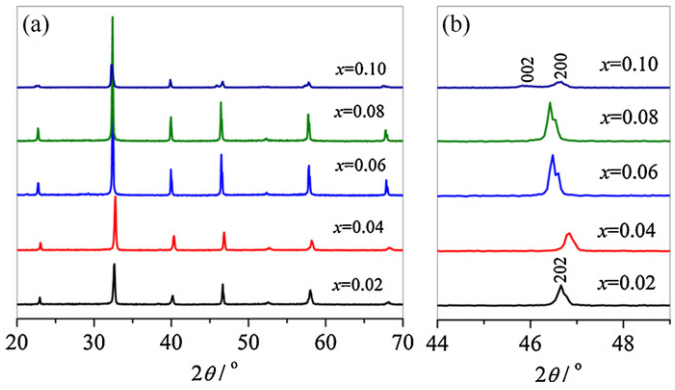

Fig. 2. XRD patterns of BNT–BT–BAT-x/0.04 ceramics in the 2θ range: (a) 20–70° and (b) 38–48°.

(99.8%), and Ag_2O (99%) were selected as the starting raw materials. The powders in the stoichiometric ratio of the compositions were mixed by ball milling for 6 h with a vibratory mill. Then the mixture was calcined at 900–950 °C for 2 h. The synthesized powders were again ball milled, granulated, and pressed into discs by dry pressuring with diameters of 13 mm and thicknesses of 1.2 mm. The compacted disks were sintered in air at 1150–1200 °C for 2 h. Silver slurry was coated on both sides of the discs and then treated at 700 °C as electrodes. The specimens were poled in silicone oil at room temperature under 4 kV/mm for 20 min.

The bulk densities of the sintered samples were measured by Archimedes' method. The microstructures were observed using scanning electron microscopy

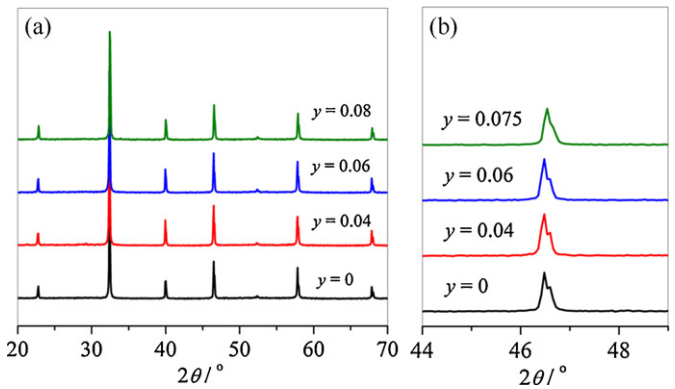

Fig. 3. XRD patterns of BNT–BT–BAT-0.06/y ceramics in the 2θ range: (a) 20–70° and (b) 38–48°.

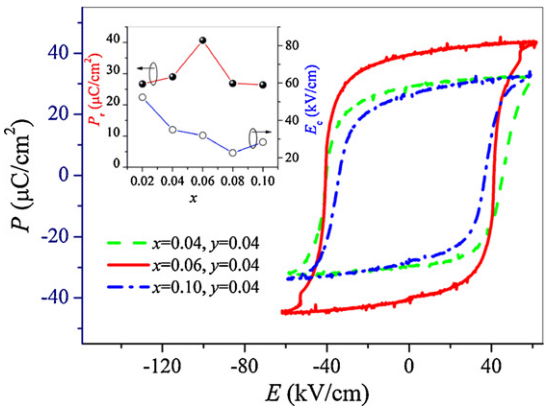

Fig. 4. P–E hysteresis loops of BNT–BT–BAT-x/0.04 ceramics with x = 0.04, 0.06, and 0.08. The inset is P_r and E_c as function of x.

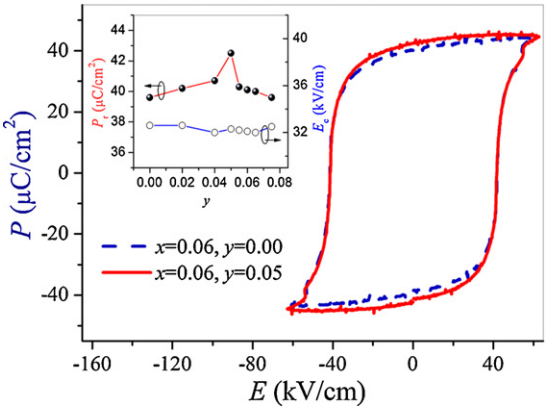

Fig. 5. P–E hysteresis loops of the BNT–BT–BAT-0.06/y ceramics with y = 0 and 0.05. The inset is P_r and E_c as function of y.

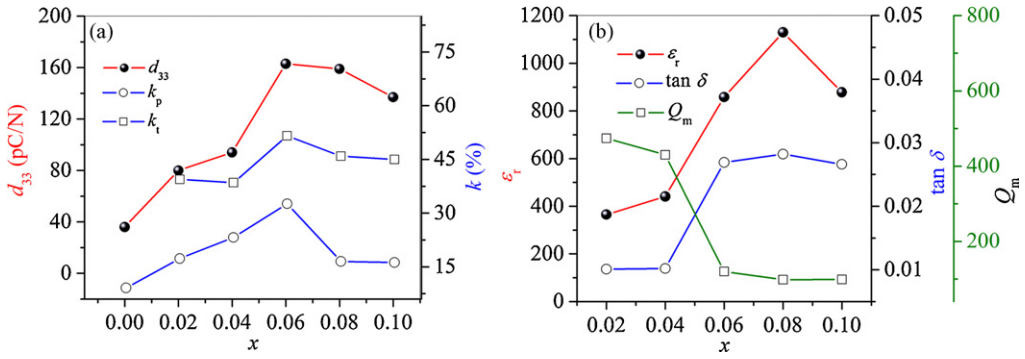

Fig. 6. (a) Piezoelectric and (b) dielectric properties of BNT–BT–BAT-x/0.04 ceramics as function of x.

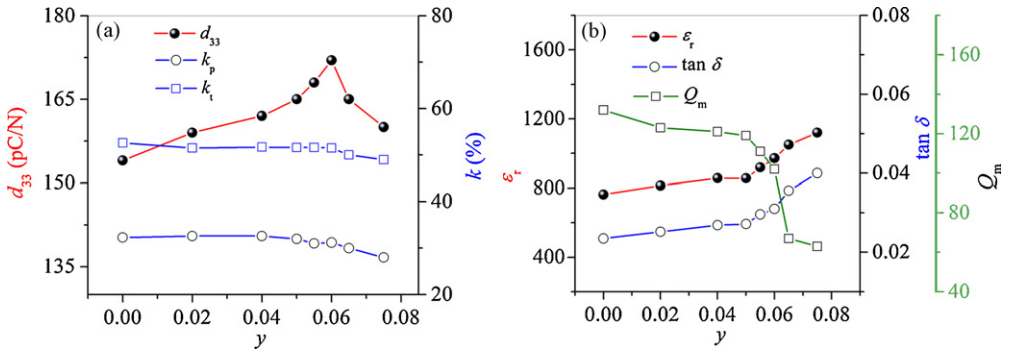

Fig. 7. (a) Piezoelectric and (b) dielectric properties of BNT–BT–BAT-0.06/y ceramics as function of y.

(SEM, JSM-5900LV). X-ray diffraction (XRD) characterization of the ceramics was performed using Cu Kα radiation in the $\theta-2\theta$ scan mode (X′ Pert PRO). The piezoelectric constant (d_{33}) was measured using a piezo-d_{33} meter (ZJ-3A). The electromechanical coupling factors (k_p and k_t) and the mechanical quality factor (Q_m) were measured and calculated by the resonance–antiresonance method using an impedance analyzer (HP 4294A) according to the IEEE standards. The temperature dependence of the k_p was measured using a programmable furnace and HP 4294A. The dielectric constant (ε_r) and dielectric loss ($\tan\delta$) of the samples were measured using an impedance analyzer (HP 4278A). The remanent polarization (P_r) and coercive field (E_c) were determined from polarization versus electric field (P–E) hysteresis loops measured by a Radiant Precision Workstation (USA).

3. Results and discussion

Fig. 1 presents the SEM micrographs of some typical compositions of the BNT–BT–BAT-x/y ceramics. It can be observed in Fig. 1 that the grain boundary of the ceramics is clear and the microstructure is dense. All the BNT–BT–BAT-x/y ceramics possess high densities of about 5.66–5.82 g/cm^3, which are more than 95.3% of the theoretical values. As shown in Fig. 1(a)–(c), the grains of the BNT–BT–BAT-x/0.04 ceramics become slightly smaller with increasing x (i.e., the amount of BT). It is thought that Ba^{2+} concentrates near grain boundaries and suppresses the grain growth in the BNT–BT–BAT-x/0.04 ceramics at a high amount of BT ($x \geq 0.10$), which is similar to that of Ba-modified PZT based ceramics [17]. Both the bulk density and relative density of the BNT–BT–BAT-x/0.04 ceramics was found to increase with increasing x. On the other hand, the grain size becomes more homogenous (~2 μm) after the addition of BAT into the BNT–BT ceramics (Fig. 1(d)–(f)). The relative density of the BNT–BT–BAT-0.06/y ceramics increases initially and then decreases with increasing y. For the ceramics with $y = 0.06$, the microstructure is uniform and the relative density reaches maximum value of 96.5%.

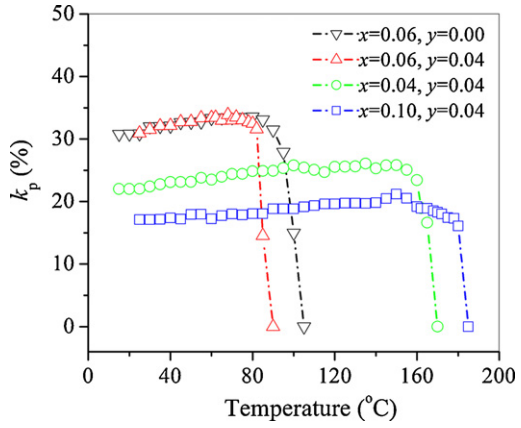

Fig. 8. Temperature dependence of k_p of BNT–BT–BAT-0.04/0.04, BNT–BT–BAT-0.06/0.00, BNT–BT–BAT-0.06/0.04, and BNT–BT–BAT-0.10/0.04 ceramics.

The XRD patterns of BNT–BT–BAT-x/0.04 and BNT–BT–BAT-0.06/y ceramics are shown in Figs. 2 and 3, respectively. All the ceramics possess a pure perovskite phase (Figs. 2(a) and 3(a)), indicating that Ba^{2+} and Ag^+ diffuse into the BNT lattices to form a solid solution. Similar to pure BNT [7,10], the BNT–BT–BAT-x/0.04 ceramics with $x < 0.06$ possess a rhombohedral symmetry, which is characterized by a single peak of (2 0 2) at about 46.5° (Fig. 2(b)). It is noted that the BNT–BT–BAT-x/0.04 ceramics starts to transform to tetragonal symmetry with further increasing x. This is evidenced by the splitting of (2 0 2) peak to (0 0 2) and (2 0 0) peaks near 46.5°. At $x = 0.10$, the lattice anisotropy c/a of the ceramics is about 1.0132. These results are very similar to the previous works on BNT–BT [5–7] and BNT–BT–$Bi_{0.5}Li_{0.5}TiO_3$ [10] system. It seems that there exists a MPB between rhombohedral and tetragonal phases of BNT–BT–BAT-x/0.04 ceramics at $x = 0.06$–0.08. On the other hand, no obvious change of the crystal structure is observed for the BNT–BT–BAT-0.06/y ceramics with increasing y (i.e., the amount of BAT), as shown in Fig. 3(b). It can be concluded that the BNT–BT–BAT-0.06/y ceramics with $y = 0$–0.075 situate near the

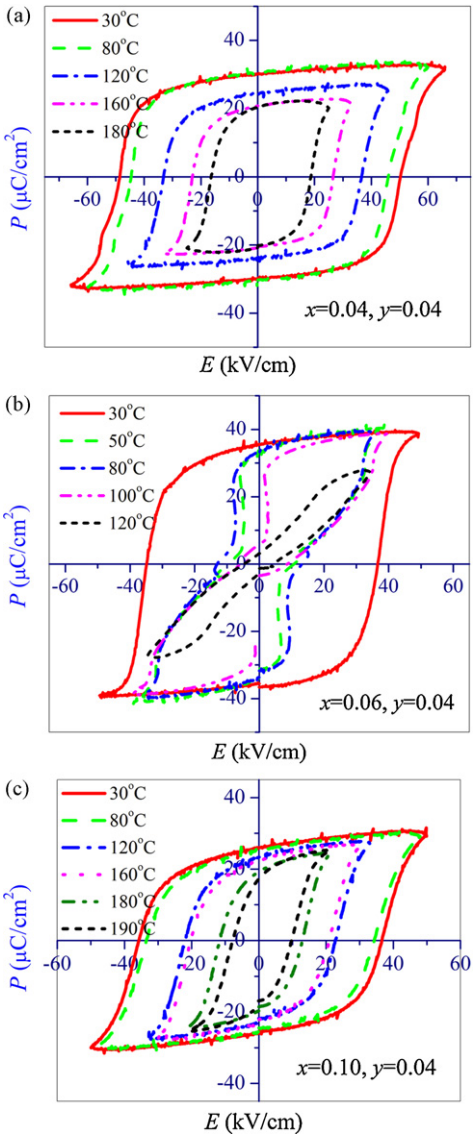

Fig. 9. *P–E* hysteresis loops of (a) BNT–BT–BAT-0.04/0.04, (b) BNT–BT–BAT-0.06/0.04, and (c) BNT–BT–BAT-0.10/0.04 ceramics at different temperatures.

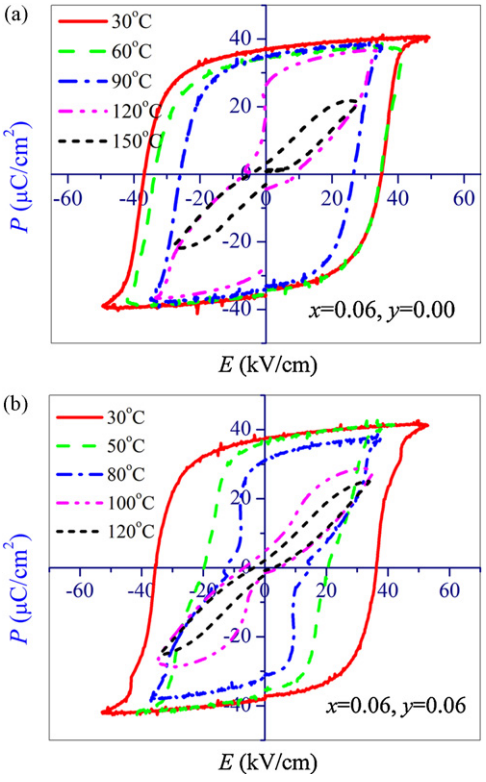

Fig. 10. *P–E* hysteresis loops of (a) BNT–BT–BAT-0.06/0.00 and (b) BNT–BT–BAT-0.06/0.06 ceramics at different temperatures.

MPB. Additional experimental data will be provided below for further discussion.

Fig. 4 shows the *P–E* hysteresis loops of the BNT–BT–BAT-*x*/0.04 ceramics with $x = 0.04, 0.06$ and 0.10, while P_r and E_c of the ceramics as a function of *x* are shown in the inset of Fig. 4. It was found that well saturated and almost rectangular loops were obtained for the BNT–BT–BAT-*x*/0.04 ceramics with $x = 0.02$–0.10. As shown in Fig. 4, the P_r of the ceramics increases with increasing *x* and reaches maximum value of 40.1 μC/cm² at $x = 0.06$. Further increasing *x* causes a decrease in the P_r. In addition, the E_c of the BNT–BT–BAT-*x*/0.04 ceramics decreases from 52.4 kV/cm to 22.6 kV/cm as *x* increases from 0.02 to 0.08 and then increases slightly with further increasing *x*. This result indicates that the incorporation of certain amount of BT into BNT–BAT ceramics can effectively decrease the E_c. The *P–E* hysteresis loops of the BNT–BT–BAT-0.06/*y* ceramics with $y = 0$ and 0.05 are shown in Fig. 5. The inset in Fig. 5 is the variations of P_r and E_c of the ceramics with *y*. It can be observed in Fig. 5 that the P_r of the BNT–BT–BAT-0.06/*y* ceramics increases slightly with increasing *y* and reaches maximum value of 42.5 μC/cm² at $y = 0.05$. The E_c of the BNT–BT–BAT-0.06/*y* ceramics remains almost unchanged (~32 kV/cm) with increasing *y*.

Fig. 6 shows (a) d_{33}, k_p, and k_t and (b) Q_m, ε_r, and $\tan\delta$ of the BNT–BT–BAT-*x*/0.04 ceramics as a function of *x*. Similar to the P_r (Fig. 4), d_{33}, k_p, and k_t of the BNT–BT–BAT-*x*/0.04 ceramics also reach the maximum values of 163 pC/N, 32.6%, and 51.6% at $x = 0.06$, respectively. It can be observed in Fig. 6(b) that ε_r and $\tan\delta$ of the BNT–BT–BAT-*x*/0.04 ceramics give their maximum values of 1130 and 0.028 at $x = 0.08$, respectively. In addition, the Q_m decreases from 474 to 98 as *x* increases from 0.02 to 0.10 (Fig. 6(b)). Fig. 7 shows (a) d_{33}, k_p, and k_t and (b) Q_m, ε_r, and $\tan\delta$ of the BNT–BT–BAT-0.06/*y* ceramics as a function of *y*. The d_{33} of the BNT–BT–BAT-0.06/*y* ceramics increases with increasing *y* and reaches maximum value of 172 pC/N at $y = 0.06$ (Fig. 7(a)). Further increasing *y* causes a decrease in the d_{33}. The k_p and k_t of the ceramics decreases slightly with increasing *y*. It can also be observed in Fig. 7(b) that the Q_m of the BNT–BT–BAT-0.06/*y* ceramics decreases while both ε_r and $\tan\delta$ increase with increasing *y*. These results indicate that the BNT–BT–BAT-0.06/0.06 ceramics possess the optimum piezoelectric properties: $d_{33} = 172$ pC/N, $k_p = 31.2\%$, $k_t = 51.5\%$.

For BNT–BT system, the MPB (at about 6 mol% of BT) separating ferroelectric rhombohedral and tetragonal phases plays an important role in the improvement of piezoelectric properties [5,6]. In this work, the enhancement in the piezoelectric and ferroelectric properties of the BNT–BT–BAT-*x*/0.04 ceramics at $x = 0.06$ can also be attributed to the existence of the MPB, because the number of possible polarization states increases at the MPB. Furthermore, the addition of BT significantly decreases the E_c of BNT–BT–BAT-*x*/0.04 ceramics can make the ceramics polarize sufficiently in the poling process, which is also helpful to the increase in piezoelectric properties. In present study, we expect that the strong hybridization between Ag and O atoms and the large distortion of Ag on the A-site can improve the ferroelectric and piezoelectric properties of BNT–BT ceramics. However, XRD analysis indicates that the addition of BAT

(y = 0–0.075) has no obvious change on the crystal structure of the BNT–BT ceramics. The effect of the structural distortion caused by Ag on the ferroelectric and piezoelectric properties might not be so significant, owing to the low concentration level of Ag ($\leq$0.0375 mol) in this system. Compared with BNT–BT ceramics (d_{33} = 154 pC/N), BAT-modified BNT–BT ceramics (i.e., BNT–BT–BAT-0.06/y) exhibit the higher piezoelectric properties (d_{33} = 172 pC/N), which should be mainly attributed to the improvement of densification (Fig. 1(d)–(f)). Another possible reason for the increase of d_{33} with increasing y may partly be attributed to the higher ε_r (~972) and larger P_r (~42.5 μC/cm^2) as compared with the BNT–BT ceramics ($\varepsilon_r \sim 763$, $P_r \sim 39.6$ μC/cm^2), because the d_{33} is proportional to both the polarization and dielectric constant [18].

It is very important to study the depolarization temperature (T_d) of BNT-based ceramics from the viewpoint of device applications. In present work, the T_d was determined from the temperature dependence of piezoelectric properties. Fig. 8 shows the temperature dependence of k_p of the BNT–BT–BAT-0.06/0.00, BNT–BT–BAT-0.04/0.04, BNT–BT–BAT-0.06/0.04, and BNT–BT–BAT-0.10/0.04 ceramics. For the BNT–BT–BAT-0.06/0.00 ceramics, it can be observed in Fig. 8 that the k_p remains almost unchanged with increasing temperature up to 95 °C. Further increasing temperature causes a sharp decline in the k_p. When the temperature reaches 105 °C, the piezoelectricity almost disappears and the ceramics are depolarized. The T_d (~105 °C) of the BNT–BT–BAT-0.06/0.00 ceramics coincides with the results obtained by Chu et al [6]. Similar curves of k_p versus temperature have also been observed in other BNT–BT–BAT-x/y ceramics. It is found that the T_d of BNT–BT–BAT-x/0.04 ceramics decreases with increasing x up to 0.06 and then increases with further increasing x. The T_d is about 170 °C, 90 °C, 120 °C, and 185 °C for the BNT–BT–BAT-x/0.04 ceramics with x = 0.04, 0.06, 0.08, and 0.10, respectively. It is worth noting that the BNT–BT–BAT-x/y ceramics with rhombohedral (x = 0.02–0.04) or tetragonal (x = 0.10) symmetry possess the higher T_d values than that of the MPB compositions (x = 0.06–0.08). Similar phenomenon has also been observed in BNT–BT [5–7] and BNT–BKT [8,19] system. In particular, the BNT–BT–BAT-0.04/0.04 ceramics which show good electrical properties (Q_m = 430, k_p = 23.2%, d_{33} = 94 pC/N, and P_r = 29.0 μC/cm^2) at room temperature, possess a high T_d of 170 °C. These results indicate that the BNT–BT–BAT-0.04/0.04 is a promising candidate material for high-power applications [19]. On the other hand, the T_d of the BNT–BT–BAT-0.06/y ceramics decreases slightly with increasing y. At x = 0.06, the T_d of the sample decreases to about 85 °C.

Fig. 9(a)–(c) shows the P–E hysteresis loops of BNT–BT–BAT-x/0.04 ceramics with x = 0.04, 0.06 and 0.10 at different temperatures, respectively. As shown in Fig. 9(a), the loop of typical ferroelectric feature can be observed at up to 180 °C for the BNT–BT–BAT-0.04/0.04 ceramics. This result is consistent with that obtained from temperature dependence of the piezoelectric properties (Fig. 8). It can be noted in Fig. 9(b) that the loop of BNT–BT–BAT-0.06/0.04 ceramics appears to form double-like P–E hysteresis loop with increasing temperature. The ferroelectricity of the ceramics becomes very weak (P_r = 3.49 μC/cm^2) when the temperature reaches 100 °C. Similar double-like P–E hysteresis loops are also observed in other BNT–BT–BAT-0.06/y ceramics, as shown in Fig. 10(a) and (b), respectively. These results indicate that the BNT–BT–BAT-x/y ceramics exhibit deformed P–E hysteresis loops at temperatures near T_d. T_d is traditionally thought to indicate a phase transition from ferroelectric to antiferroelectric [5]. At higher temperatures, the BNT–BT–BAT-x/y ceramics still exhibit ferroelectric-like characteristics (P_r = 2–5 μC/cm^2), not typically antiferroelectric-like (double P–E loops). Recently, Tai et al. [20] confirmed that the ferroelectric–antiferroelectric transition does not occur in the BNT–BKT–$Bi_{0.5}Li_{0.5}TiO_3$–BT ceramics near T_d. Similar deformed hysteresis loops have also been observed in other BNT-based ceramics, such as BNT–BT–$Bi_{0.5}Li_{0.5}TiO_3$ [10] and $(Na_{0.5}Bi_{0.5})_{0.70}Ba_{0.30}TiO_3$ [21] system, which was suggested to result from the coexistence of polar and microscopically non-polar phases [10,21,22]. In this work, the poled BNT–BT–BAT-x/y ceramics had d_{33} values of 5–15 pC/N after they were annealed above T_d for 30 min, which is also an indication for the existence of polar phases at temperatures above T_d. So our results suggest that the polar and non-polar phases may coexist in the BNT–BT–BAT-x/y ceramics at temperatures above T_d.

4. Conclusions

BNT–BT–BAT-x/y lead-free piezoelectric ceramics were prepared by the conventional solid-state sintering. The phase structure, microstructure, piezoelectric, and ferroelectric properties of the ceramics were studied. SEM analysis shows that the addition of BT inhibits the grain growth of BNT–BAT ceramics. The MPB between rhombohedral and tetragonal phases is identified at x = 0.06–0.08 for the BNT–BT–BAT-x/0.04 ceramics. The addition of BAT has no obvious change on the crystal structure of the BNT–BT ceramics while it causes the grain size of ceramics to become more homogenous. The BNT–BT–BAT-x/y ceramics exhibit optimum electrical properties ($d_{33} \sim 172$ pC/N, $k_p \sim 32.6\%$, k_t = 52.6%, $P_r \sim 42.5$ μC/cm^2, and $E_c \sim 32$ kV/cm) in the MPB region. The dependences of k_p and P–E hysteresis loops on temperature show that the T_d of BNT–BT–BAT-0.06/y ceramics decreases with increasing y. It also reveals that the polar and non-polar phases may coexist in the BNT–BT–BAT-x/y ceramics at temperatures above T_d.

Acknowledgements

This work was supported by NSFC Projects (50572066, 10775113), and the Doctorial Project of Southwest University of Science and Technology (08zx0112).

References

[1] E. Cross, Nature 432 (2004) 24–25.
[2] Y. Saito, H. Takao, T. Tani, T. Nonoyama, K. Takatori, T. Homma, T. Nagaya, M. Nakamura, Nature 432 (2004) 84–87.
[3] G.A. Smolenskii, V.A. isupov, A.I. Agranovskaya, N.N. Krainik, Sov. Phys. Solid State 2 (1961) 2651–2654.
[4] Y. Hiruma, H. Nagata, T. Takenaka, J. Appl. Phys. 105 (2009) 084112.
[5] T. Takenaka, K. Maruyama, K. Sakata, Jpn. J. Appl. Phys. 30 (1991) 2236–2239.
[6] B.J. Chu, D.R. Chen, G.R. Li, Q.R. Yin, J. Eur. Ceram. Soc. 22 (2002) 2115–2121.
[7] C.G. Xu, D.M. Lin, K.W. Kwok, Solid State Sci. 10 (2008) 934–940.
[8] A. Sasaki, T. Chiba, Y. Mamiya, E. Otsuki, Jpn. J. Appl. Phys. 38 (1999) 5564–5567.
[9] H. Yu, Z.G. Ye, Appl. Phys. Lett. 93 (2008) 112902.
[10] D.M. Lin, K.W. Kwok, H.L.W. Chan, Solid State Ionics 178 (2008) 1930–1937.
[11] A.B. Kounga, S.T. Zhang, W. Jo, T. Granzow, J. Rödel, Appl. Phys. Lett. 85 (2004) 91–93.
[12] I. Grinberg, A.M. Rappe, Appl. Phys. Lett. 85 (2004) 1760–1762.
[13] D. Fu, M. Endo, H. Taniguchi, T. Taniyama, M. Itoh, Appl. Phys. Lett. 90 (2007) 252907.
[14] R. Wang, K. Kobashi, M. Itoh, Y.J. Shan, T. Nakamura, Ferroelectrics 264 (2001) 127–132.
[15] J.-H. Park, P.M. Woodward, J.B. Parise, R.J. Reeder, I. Lubomirsky, O. Stafsudd, Chem. Mater. 11 (1999) 177–183.
[16] Y. Lu, Y. Li, D. Wang, Q. Yin, Ferroelectrics 358 (2007) 109–116.
[17] K. Ramam, M. Lopez, J. Phys. D: Appl. Phys. 39 (2006) 4466–4471.
[18] D. Damjanovic, Rep. Prog. Phys. 61 (1998) 1267–1324.
[19] T. Takenaka, H. Nagata, Y. Hiruma, IEEE Trans. Ultrason. Ferroelectr. Freq. Control 56 (2009) 1595–1612.
[20] C.W. Tai, S.H. Choy, H.L.W. Chan, J. Am. Ceram. Soc. 91 (2008) 3335–3341.
[21] J. Suchanicz, J. Kusz, H. Böhm, H. Duda, J.P. Mercurio, J. Eur. Ceram. Soc. 22 (2003) 1559–1564.
[22] J. Suchanicz, Ferroelectrics 209 (1998) 561–568.